

Tweaking baseline constellations for airborne SAR tomography and InSAR: an experimental study at L- and P-bands

Othmar Frey

Earth Observation & Remote Sensing, ETH Zurich, Switzerland / Gamma Remote Sensing, Gümliigen, Switzerland
Email: ofrey@ethz.ch

Erich Meier

Remote Sensing Laboratories, University of Zurich, Switzerland

Irena Hajsek

Earth Observation & Remote Sensing, ETH Zurich, Switzerland / German Aerospace Center - DLR, Germany

Abstract

A notable obstacle hindering widespread application of SAR tomography for 3D mapping of vegetation is the relatively large number of acquisitions that are needed to obtain a high resolution and a good rejection of spurious responses in the direction perpendicular to the line of sight. In this paper, we discuss the impact of different baseline constellations on 3-D mapping of vegetation volumes and the underlying topography in terms of tomographic focusing as well as classical single-baseline repeat-pass interferometry. The effects are studied using two airborne tomography data sets at L- and P-bands.

1 Introduction

SAR tomography is a maturing technique for 3-D mapping in the microwave domain [1–13] with a notable difficulty, in practice, given by the relatively large number of acquisitions that are needed to obtain a high resolution and a good rejection of spurious signals. Suggestions to reduce the number of acquisitions were brought forward, recently, e.g. by [14].

In this paper, we investigate, experimentally, which of the (available) baseline constellations are useful in the context of robust Capon beamforming and MUSIC focusing of a forested area under the following conditions: (1) when the number of acquisitions is reduced and (2) without introducing a model for the vegetation volume and the underlying ground. The experimental airborne tomography data sets used for this purpose are summarized in Table 1. A detailed description of the data sets, as well as the time-domain-based tomographic focusing methods employed, are found in [12] and [13], respectively.

For operational data acquisition scenarios not only the number of baselines should be reduced but also a baseline configuration that is optimal with respect to the mission's purpose has to be found; such as the extraction of a digital elevation model below forest canopy, or the extraction of vegetation parameters by means of multibaseline focusing and analysis of SAR tomography data.

| | P-band | L-band |
|---|---------|---------|
| Carrier frequency | 350 MHz | 1.3 GHz |
| Chirp bandwidth | 70 MHz | 94 MHz |
| Sampling rate | 100 MHz | 100 MHz |
| PRF | 500 Hz | 400 Hz |
| Ground speed | 90 m/s | 90 m/s |
| No. of data tracks | 11+1 | 16+1 |
| Nominal track spacing d_n | 57 m | 14 m |
| Horizontal baselines | 40 m | 10 m |
| Vertical baselines | 40 m | 10 m |
| Synthetic aperture in normal direction L | 570 m | 210 m |
| Nominal resolution in normal direction δ_n | 3 m | 2 m |
| Approx. unambiguous height H | 30 m | 30 m |

Table 1: E-SAR system specifications and nominal parameters of the tomographic acquisition patterns for both multibaseline data sets at P-band and L-band.

With the help of the two multibaseline SAR data sets at L- and P-bands, we extend our analysis regarding the potential variation of the measured backscattering values of a forest as a function of total baseline length and a varying mean incidence angle.

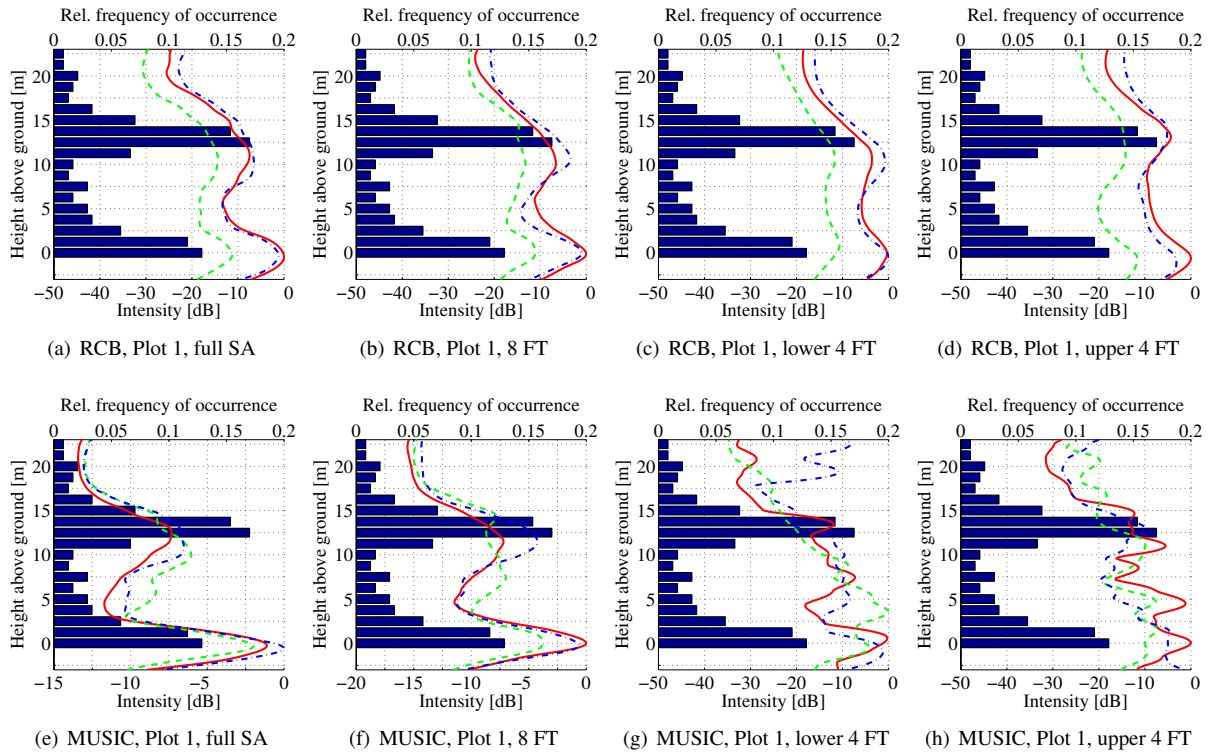


Figure 1: Vertical profiles of relative intensities from L-band tomographic data of a forest (Plot 1) averaged over a circular sample plot of 300m² for the polarimetric channels HH (—), HV (---), and VV (·-·), RCB, and MUSIC. In each row, the following sequence of number of flight tracks (FT) is given, from left to right: (1) full SA (16 FT), (2) approx. half the SA (8 FT), (3) the lower 4 flight tracks, and (4) the upper 4 flight tracks. For comparison, histograms of height differences between the ALS DSM and the ALS DEM are underlaid as an external estimate of the distribution of tree heights.

2 Results

In Figs. 1 & 2, plots of vertical profiles of intensities are presented (HH, HV, and VV channels) at L- and P-bands. The focusing methods that were applied are robust Capon beamforming and MUSIC beamforming. Each row contains, from left to right, the following sequence of number of flight tracks (FT) used in tomographic focusing: (1) full synthetic aperture (L-band: 16 FT, P-band: 11 FT), (2) approx. half the synthetic aperture (L-band: 8 FT, P-band: 6 FT), (3) the lower four flight tracks, and (4) the upper four flight tracks (see [13], Fig. 1 for a detailed description of the acquisition geometry). Fig. 3 contains coherence and phase histograms for two different baselines and varying incidence angles from interferometric pairs of a forested area at P-band.

3 Discussion

The tomographic intensity profiles remain rather stable even if the total number of flight tracks is halved to 8 FT, for L-band, and to 6 FT, for P-band, respectively. The intensity profiles are also stable using both focusing methods, RCB and MUSIC. However, if the number of flight tracks is further reduced to four acquisitions tomographic

focusing using the MUSIC algorithm delivers erroneous vertical profiles of intensities for case (3) and (4) at L-band. RCB shows a more robust behavior towards a reduction of samples. As MUSIC is a subspace method, which relies upon a separation of signal space and noise space, a total number of only four flight tracks does not provide an adequate number of samples in cases of distributed scatterers, or if several backscattering sources occur within a range resolution cell. The degradation is less pronounced at P-band, presumably, due to the lower number of dominant scattering sources occurring within one slant-range resolution cell at that frequency.

The two smallest subapertures (4 flight tracks) consisting of the outermost flight tracks can also be used to indicate whether a change of the mean incidence angle of a tomographic acquisition is reflected in the vertical profiles of intensities. Since for MUSIC beamforming, the tomographic signal suffers from considerable degradation, in the case where only 4 flight tracks are used, only the RCB-based results are taken into account, here: for the given sample plot 1, the vertical profiles do not change much.

In addition, the two multibaseline data sets provide an opportunity to assess the effect of variations of baselines or incidence angles on repeat-pass interferometry. In Fig. 3, an example of coherence histograms and respective inter-

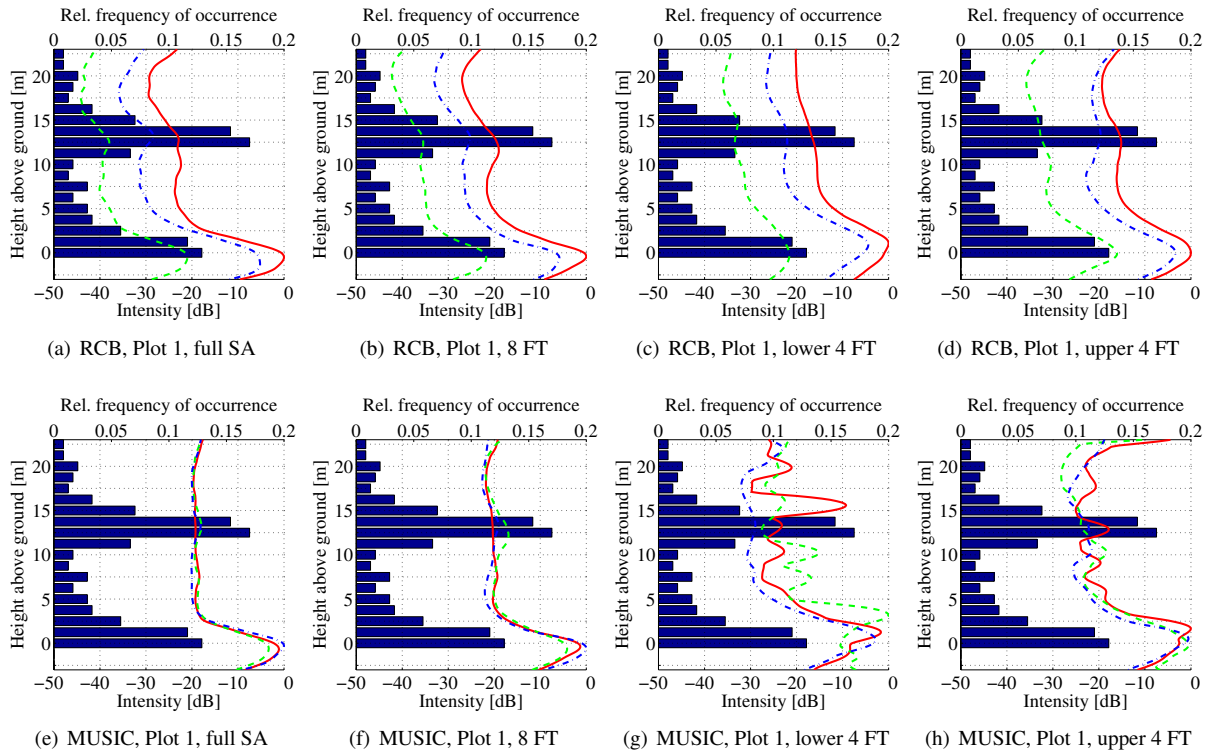


Figure 2: Vertical profiles of relative intensities from P-band tomographic data of a forest (Plot 1) averaged over a circular sample plot of 300m² for the polarimetric channels HH (—), HV (---), and VV (-·-), RCB, and MUSIC. In each row, the following sequence of number of flight tracks (FT) is given, from left to right: (1) full SA (11 FT), (2) approx. half the SA (6 FT), (3) the lower 4 flight tracks, and (4) the upper 4 flight tracks. For comparison, histograms of height differences between the ALS DSM and the ALS DEM are underlaid as an external estimate of the distribution of tree heights.

ferometric phase histograms (relative to the topography) is given for the VV-channel of interferometric pairs taken from the P-band data set. It is interesting to note that there is a tendency to phase estimates closer to the topography under forest cover in the case where the sensor is looking down steeply (near range) as well as for the larger baseline, although the coherence is generally lower in these cases.

Acknowledgment

The authors would like to thank the procurement and technology center of the Swiss Federal Department of Defense (armasuisse W+T), in particular P. Wellig, for supporting this work. They would also like to thank the E-SAR/F-SAR team at the Department of SAR Technology, German Aerospace Center (DLR) for their ongoing cooperation.

References

- [1] A. Reigber and A. Moreira, “First Demonstration of Airborne SAR Tomography Using Multibaseline L-Band Data,” *IEEE Transactions on Geoscience and Remote Sensing*, vol. 38, no. 5, pp. 2142–2152, 2000.
- [2] F. Lombardini and A. Reigber, “Adaptive spectral estimation for multibaseline SAR tomography with airborne L-band data,” in *IEEE International Geoscience and Remote Sensing Symposium, IGARSS '03.*, vol. 3, 2003, pp. 2014–2016.
- [3] A. Reigber, M. Neumann, S. Guillaso, S. Sauer, and L. Ferro-Famil, “Evaluating PolInSAR parameter estimation using tomographic imaging results,” in *Proc. European Radar Conf.*, 2005, pp. 189–192.
- [4] M. Nannini and R. Scheiber, “A time domain beamforming algorithm for sar tomography,” in *Proc. of EUSAR 2006 - 6th European Conference on Synthetic Aperture Radar*, 2006.
- [5] O. Frey, F. Morsdorf, and E. Meier, “Tomographic Processing of Multi-Baseline P-Band SAR Data for Imaging of a Forested Area,” in *Proc. IEEE Int. Geosci. Remote Sens. Symp.*, 2007.
- [6] O. Frey, F. Morsdorf, and E. Meier, “Tomographic Imaging of a Forested Area By Airborne Multi-Baseline P-Band SAR,” *Sensors, Special Issue on Synthetic Aperture Radar*, vol. 8, no. 9, pp. 5884–5896, sep 2008.

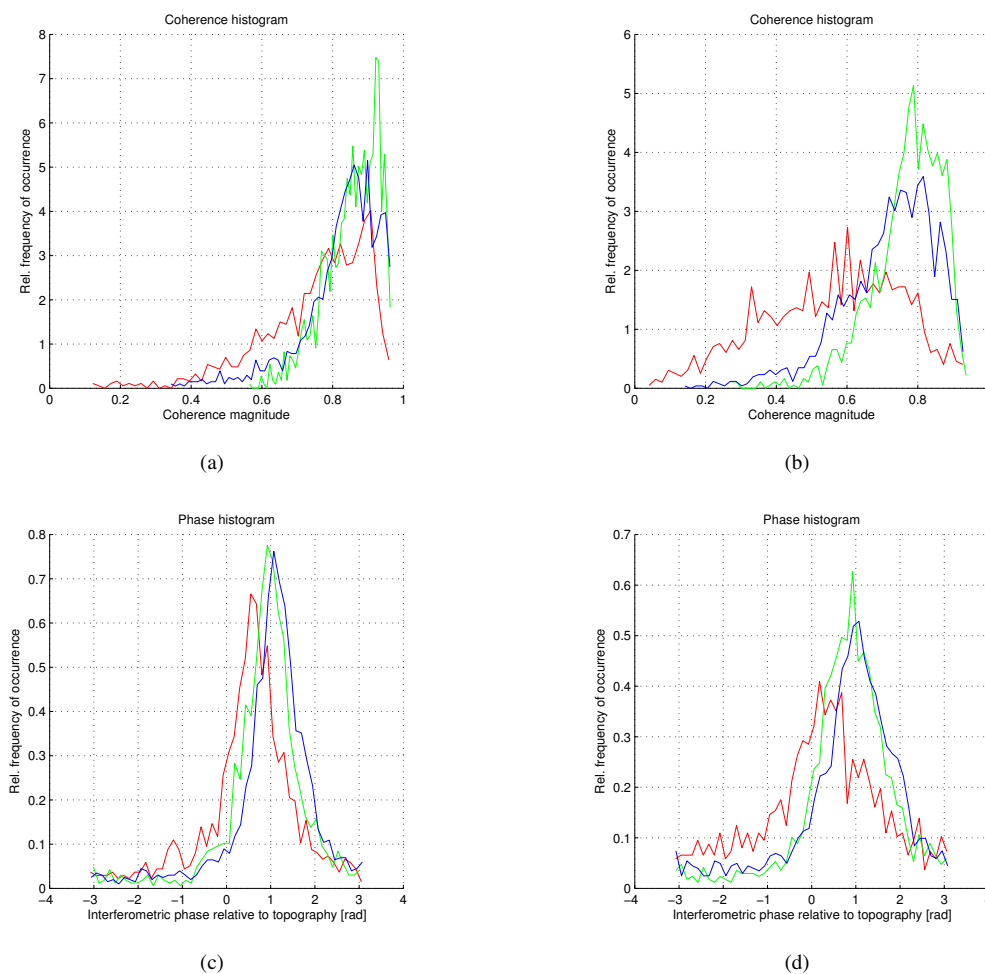


Figure 3: Coherence histograms and histograms of interferometric phase relative to the topography within the forested area for P-band, VV-Channel. Red: Near range, green: mid range, blue: far range. Coherence histograms for nominal baselines of (a) around 57m and (b) around 114m. The respective phase histograms relative to topography are given in (c) and (d).

- [7] M. Nannini, R. Scheiber, and A. Moreira, “Estimation of the minimum number of tracks for SAR tomography,” *IEEE Trans. Geosci. Remote Sens.*, vol. 47, no. 2, pp. 531–543, Feb. 2009.
- [8] S. Tebaldini, “Algebraic synthesis of forest scenarios from multibaseline PolInSAR data,” *IEEE Trans. Geosci. Remote Sens.*, vol. 47, no. 12, pp. 4132–4142, Dec. 2009.
- [9] F. Lombardini, F. Cai, and M. Pardini, “Tomographic analyses of non-stationary volumetric scattering,” in *Proc. EUSAR*, June 2010, pp. 1–4.
- [10] Y. Huang, L. Ferro-Famil, and A. Reigber, “Under foliage object imaging using SAR tomography and polarimetric spectral estimators,” in *Proc. EUSAR*, June 2010, pp. 1–4.
- [11] S. Tebaldini, “Single and multipolarimetric SAR tomography of forested areas: A parametric approach,” *IEEE Trans. Geosci. Remote Sens.*, vol. 48, no. 5, pp. 2375–2387, May 2010.
- [12] O. Frey and E. Meier, “3-D time-domain SAR imaging of a forest using airborne multibaseline data at L- and P-bands,” *IEEE Trans. Geosci. Remote Sens.*, vol. 49, no. 10, pp. 3660–3664, Oct. 2011.
- [13] O. Frey and E. Meier, “Analyzing tomographic SAR data of a forest with respect to frequency, polarization, and focusing technique,” *IEEE Trans. Geosci. Remote Sens.*, vol. 49, no. 10, pp. 3648–3659, Oct. 2011.
- [14] V. Severino, M. Nannini, A. Reigber, R. Scheiber, A. Capozzoli, G. D’Elia, A. Liseno, and P. Vinetti, “An approach to SAR tomography with limited number of tracks,” in *IEEE Int. Geosci. Remote Sens. Symp.*, vol. 4, July 2009, pp. 216–219.